Available online at www.sciencedirect.com
ScienceDirect
European Journal of Protistology 44 (2008) 55–70
European Journal of PROTISTOLOGY
www.elsevier.de/ejop

Ultrastructure of a novel tube-forming, intracellular parasite of dinoflagellates: *Parvilucifera prorocentri* sp. nov. (Alveolata, Myzozoa)

Brian S. Leander*, Mona Hoppenrath

Canadian Institute for Advanced Research, Program in Integrated Microbial Biodiversity, Departments of Botany and Zoology, University of British Columbia, Vancouver, BC, Canada V6T 1Z4

Received 18 April 2007; received in revised form 16 August 2007; accepted 21 August 2007

Abstract

We have characterized the intracellular development and ultrastructure of a novel parasite that infected the marine benthic dinoflagellate *Prorocentrum fukuyoi*. The parasite possessed a combination of features described for perkinsids and syndineans, and also possessed novel characters associated with its parasitic life cycle. Reniform zoospores, about 4 μm long, possessed a transverse flagellum, alveoli, a refractile body, a mitochondrion with tubular cristae, a syndinean-like nucleus with condensed chromatin, micronemes, bipartite trichocysts with square profiles (absent in perkinsids) and oblong microbodies. Like *Parvilucifera*, the zoospores also possessed a shorter posterior flagellum, a heteromorphic pair of central microtubules in the anterior axoneme and a reduced pseudoconoid positioned directly above an orthogonal pair of basal bodies. Early developmental stages consisted of a sporangium about 5–15 μm in diam that contained spherical bodies and amorphous spaces. The undifferentiated sporangium increased to about 20–25 μm in diam before being enveloped by a wall with a convoluted mid-layer. The sporangium differentiated into an unordered mass of zoospores that escaped from the cyst through a pronounced germ tube about 4–5 μm in diam and 10–15 μm long. Weakly developed germ tubes have been described in *Perkinsus* but are absent altogether in *Parvilucifera* and syndineans. Comparison of these data with other myzozoans led us to classify the parasite as *Parvilucifera prorocentri* sp. nov., Myzozoa. Although we were hesitant to erect a new genus name in the absence of molecular sequence data, our ultrastructural data strongly indicated that this parasite is most closely related to perkinsids and syndineans, and represents an intriguing candidate for the cellular identity of a major subclade of Group I alveolates.

Keywords: *Colpodella*; Group I alveolates; *Parvilucifera*; *Perkinsus*; *Syndinium*; Ultrastructure

Introduction

The Myzozoa is a clade of alveolates consisting of the most recent common ancestor of apicomplexans and dinoflagellates and all of its descendants. An improved understanding of myzozoan lineages that do not fall neatly within the Apicomplexa and the Dinoflagellata *sensu stricto* is critical for inferring the earliest stages of alveolate evolution (Cavalier-Smith and Chao 2004; Kuvardina et al. 2002; Leander and Keeling 2003; Siddall et al. 2001). Several genera of predatory and parasitic flagellates have been shown to diverge near the phylogenetic origins of dinoflagellates and apicomplexan parasites, namely *Alphamonas*, *Chilovora*, *Colpodella*, *Duboscquella*, *Parvilucifera*, *Perkinsus*, *Rastrimonas*

*Corresponding author. Tel.: 1 604 822 2474; fax: 1 604 822 6089.
E-mail address: bleander@interchange.ubc.ca (B.S. Leander).

0932-4739/$ - see front matter © 2007 Elsevier GmbH. All rights reserved.
doi:10.1016/j.ejop.2007.08.004

(formerly *Cryptophagus*) and *Voromonas* (Brugerolle 2002, 2003; Cavalier-Smith and Chao 2004; Harada et al. 2007; Kuvardina et al. 2002; Leander and Keeling 2004; Leander et al. 2003; Norén et al. 1999; Saldarriaga et al. 2003; Siddall et al. 1997). These organisms share several homologous characteristics associated with myzocytotic modes of feeding (or intracellular infection) that are inferred to be synapomorphic for the Myzozoa, such as an apical complex consisting of micronemes, rhoptry-like extrusomes and a pseudoconoid (syn. "open" conoid). The apical complex was retained and further modified along the apicomplexan lineage (e.g. the evolution of a "closed" conoid) and appears to have been secondarily lost along the dinoflagellate lineage. However, components of the apical complex are present in several parasitic sister groups to the "core" dinoflagellates, such as perkinsids.

Marine environmental sequencing surveys using small subunit (SSU) rDNA have demonstrated two large and diverse groups of alveolates that show close phylogenetic affinity to perkinsids and "core" dinoflagellates, namely Group I alveolates and Group II alveolates (Diez et al. 2001; Dolven et al. 2007; Groisillier et al. 2006; López-García et al. 2001; Moon-van der Staay et al. 2001; Moreira and López-García 2002; Takishita et al. 2007; Worden 2006). Group I alveolates have been shown to include parasites of tintinnid ciliates like *Duboscquella* (Harada et al. 2007), and there is molecular phylogenetic evidence that at least some of these alveolates are parasites of "radiolarians" (Dolven et al. 2007). Group II alveolates have been identified as syndineans, a group consisting of several different genera of marine parasites, such as *Amoebophrya*, *Hematodinium* and *Syndinium* (Coats 1999; Moon-van der Staay et al. 2001; Moreira and López-García 2002; Saldarriaga et al. 2004; Skovgaard et al. 2005). As in perkinsids, the life cycle of syndineans consists of zoospores (syn. zooids) that penetrate a host (e.g. copepods, polycystines and dinoflagellates) and develop into an undifferentiated sporangium (syn. plasmodium) (Azevedo 1989; Azevedo et al. 1990; Blackbourn et al. 1998; Dungan and Reece 2006; Fritz and Nass 1992; Manier et al. 1971; Perkins 1976). The growing sporangium eventually destroys the internal compartment of the host and differentiates into many minute zoospores (ranging from about 3 to 20 μm in length, depending on the species) that escape the host in order to infect a new one. Whether or not a sexual phase involving anisogametes takes place during the zoospore stage between host infections is poorly understood (Cachon and Cachon 1987; Coats 1999). Collectively, these parasites are widely distributed in marine environments, infect a broad range of hosts (e.g. dinoflagellates) and play important roles in the ecological dynamics of plankton communities (Park et al. 2004).

We have discovered an intracellular parasite of the marine benthic, sand-dwelling dinoflagellate *Prorocentrum fukuyoi* Murray et al. (2007) that shares several features described for perkinsids and syndineans, but also possesses novel characters associated with its parasitic life cycle. Our objective in this paper is to characterize the intracellular development and ultrastructure of this parasite using light and electron microscopy. Comparison of these data with other described myzozoan predators and parasites (e.g. colpodellids, perkinsids and syndineans) led us to propose a new species name for this novel lineage, conservatively within the genus *Parvilucifera*.

Materials and methods

Collection of organisms

Sand samples containing *Prorocentrum fukuyoi* Murray et al., 2007 were collected with a spoon during low tide at Centennial Beach, Boundary Bay, BC, Canada during the summer and fall months of 2004–2006 (see also Hoppenrath and Leander 2006). The sample used for this investigation was taken on September 5, 2005. The sand samples were transported directly to the laboratory, and the flagellates were separated from the sand by extraction through a fine filter (mesh size 45 μm) using melting seawater-ice (Uhlig 1964). The flagellates accumulated in a Petri dish beneath the filter and were identified at 40× to 250× magnification. The original extraction was kept as raw culture, supplemented with filtered seawater and stored in the laboratory at about 17 °C under normal daylight conditions. The "culture" was examined periodically, and intracellular parasitic infections of the *P. fukuyoi* were apparent following 3–4 weeks of incubation.

Light microscopy

Infected cells were observed directly with a Leica DMIL inverted microscope and observations with differential interference contrast (DIC) were made using a Zeiss Axioplan 2 imaging microscope. Digital images were recorded in colour.

Scanning electron microscopy

An extraction sample containing mainly infected cells was fixed with two drops of acidic Lugol's solution over night. The fixed cells were placed on a 5-μm polycarbonate membrane filter (Corning Separations Div., Acton, MA) and dehydrated with a series of increasing ethanol concentrations, followed by hexamethyldisilazane (HMDS). The filter was initially dried at room

temperature and then in a 60 °C oven for 5 min, mounted on an aluminium stub and sputter coated with a mixture of gold and palladium. Samples were viewed using a Hitachi S4700 Scanning Electron Microscope. SEM images were presented on a black background using Adobe Photoshop 6.0 (Adobe Systems, San Jose, CA).

Transmission electron microscopy

Infected cells were manually isolated and concentrated in Eppendorf tubes by slow centrifugation. The pellet of cells was pre-fixed with 2% (v/v) glutaraldehyde in unbuffered seawater at 4 °C for 1 h. The pellet was washed twice in unbuffered seawater before being post-fixed in 1% (w/v) OsO_4 for 1 h. The pellet was dehydrated through a graded series of ethyl alcohols, infiltrated with acetone–resin mixtures, and embedded in Epon resin. Resin blocks were polymerized at 60 °C and sectioned with a diamond knife on a Leica Ultracut UltraMicrotome. Thin sections (70–80 nm) were stained with uranyl acetate and lead citrate and viewed under a Hitachi H7600 Transmission Electron Microscope.

Results

Occurrence

Prorocentrum fukuyoi occurred in late summer and fall samples in 2004 and 2005. *Parvilucifera prorocentri* infections were first observed in September 2004. The results presented here are from a sediment sample taken in September 2005, which contained high cell concentrations of *P. fukuyoi*. The infection dominated in 3-week old raw cultures, and the highest infection rate after 4 weeks was about 95–100%. Other dinoflagellate taxa present in the sample were not infected with the parasite, namely the phototrophic taxa *Thecadinium yashimaense* Yoshimatsu, Toriumi et Dodge, *Thecadinium kofoidii* (Herdman) Larsen, *Adenoides eludens* (Herdman) Balech, *Amphidinium testudo* Herdman; and the heterotrophic taxa *Herdmania litoralis* Dodge emend. Hoppenrath, *Sinophysis stenosoma* Hoppenrath and *Amphidinium semilunatum* Herdman. The sample also contained low numbers of an undescribed *Prorocentrum* species, which were not infected at that time. Our 2006 samples contained *P. fukuyoi*, but did not contain the parasite.

Life history

Parvilucifera prorocentri infected the dinoflagellate *P. fukuyoi*, which, in the uninfected condition, contained a conspicuous pusule positioned in the upper portion of the cell (Figs 1–3). The earliest stages of infection occured in the upper region close to the periflagellar area of the host cell, opposite to the normal pusule position (Figs 1 and 4). The pusule was never seen in the host cell during the early stages of infection, suggesting that the presence and structure of the pusule is affected by the infection process. The sequence of intracellular development that occurred following the initial infection by *Parv. prorocentri* is outlined in Figs 4–12. Once a parasitic zoospore entered the host, it began to divide (Fig. 4) and formed an intracellular sporangium about 5–15 μm in diam and consisting of spherical bodies and amorphous spaces (Figs 5–6). As the sporangium began to occupy the majority of the host intracellular compartment and reached a size of 20–25 μm in diam, a robust cyst wall formed around an undifferentiated mass (Fig. 7). At this stage, the cyst wall sprouted a pronounced germ tube (syn. discharge tube) about 4–5 μm in dia. and 10–15 μm long that pierced the host cell through the suture between the left and right thecal plates (Figs 8 and 15). The germ tube initially remained closed and was capped by a dome-shaped tip (Figs 8, 9 and 18). Simultaneous with the differentiation of the sporangial mass into ovoid cells, the tip of the germ tube formed a circular opening about 4–5 μm in diameter (Figs 9–10 and 15–20). The middle stages of sporangial differentiation consisted of a central mass surrounded by ovoid cells (Fig. 9). Eventually, the entire sporangium became a dense mass of reniform cells by the time that the germ tube opened (Fig. 10). These cells became fully developed zoospores (syn. swarmer cells) that escaped from the cyst through the open germ tube (Figs 10–12). Each zoospore was relatively uniform in size and shape, about 4 μm long × 1.5 μm wide and possessed a posterior refractile body (carbohydrate grain) and a transverse (anterior) flagellum when viewed with the light microscope (Fig. 10: Inset); a second shorter (posterior) flagellum was observed with TEM (see below). By the time the mature cyst was empty of zoospores, the host cell was completely destroyed (Figs 11, 12 and 16, 17).

Some host cells contained two sporangia that were at different stages in development (Figs 13 and 14). The difference in developmental stages indicated that double sporangia were the result of independent infections of the host by different zoospores.

Ultrastructural organization

During the earliest stages of development, the sporangial envelope of *Parv. prorocentri* included a convoluted structure that interacts with the cytoplasm of the host (Figs 4, 5 and 21–24). At this time this envelope consisted of three distinct layers: an outer layer, a convoluted middle layer and an inner layer

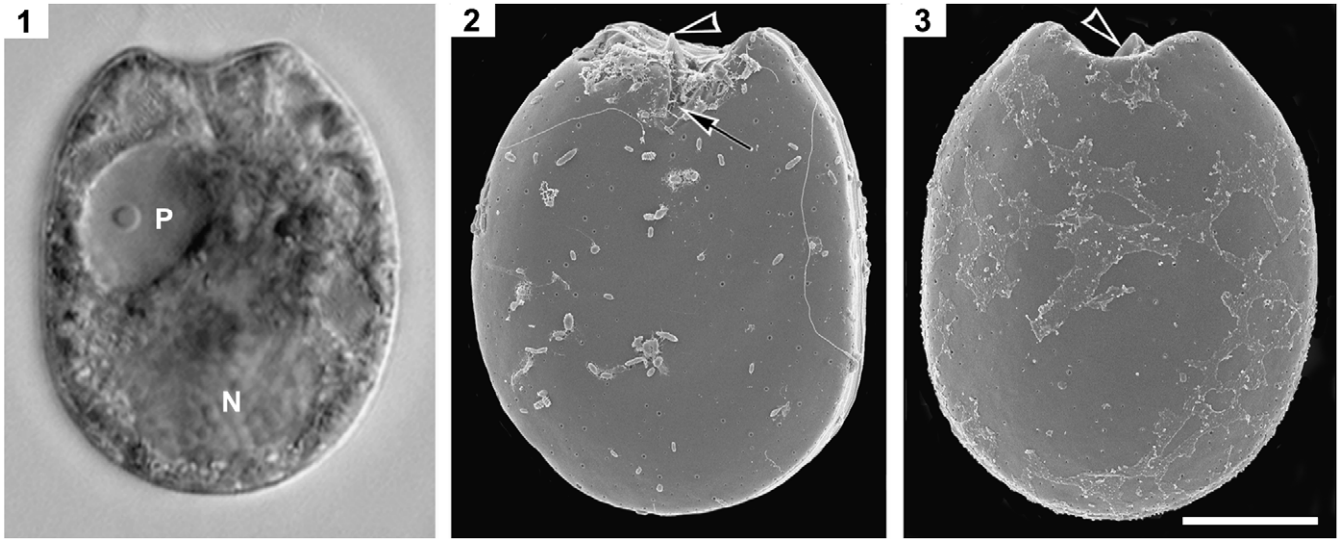

Figs 1–3. Micrographs of the dinoflagellate host, *Prorocentrum fukuyoi*. **1**. Differential interference light micrograph view from the left valve showing the pusule (p) positioned in the anterior end of the cell and the posterior nucleus (N). **2**. Scanning electron micrograph (SEM) showing the right valve of the host, the V-shaped periflagellar area (arrow) and the spine-like wing (arrowhead). **3**. SEM showing the left valve of the host and the spine-like wing (arrowhead). All figures are at the same scale (Scale bar = 10 μm).

(Figs 21–24). During the early to middle stages of development, the sporangia consisted of undifferentiated cytoplasm containing a few nuclei without condensed chromatin, lipid droplets, rough endoplasmic reticulum, mitochondria with tubular cristae, Golgi bodies and amorphous spaces (Figs 6, 7, 23 and 25–27). Higher magnification TEMs also demonstrated the presence of bipartite trichocysts (Fig. 27).

TEMs through cysts at middle to late stages in development demonstrated a more differentiated cytoplasm within a thicker cyst wall (Figs 28–30). The cytoplasm contained amorphous spaces and many nuclei with condensed chromatin that subtended the nuclear envelope (Fig. 28). The progression of nuclear development consisted of, first, nuclei without condensed chromatin; second, nuclei with intermediately condensed chromatin that was reticulate and broadly distributed; and third, nuclei with a conspicuous nucleolus and condensed chromatin distributed beneath the nuclear envelope (Figs 25, 26 and 30–32). The intracellular cysts were often indented (Fig. 25). Higher magnification TEMs demonstrated alveolar vesicles that subtended the cyst wall, mitochondria with tubular cristae, trichocysts and fully developed axonemes (Figs 29–34). The trichocysts were enveloped by a membrane and consisted of two main components: a ''head'' (syn. twisted filaments) and a ''body'' (syn. basal rod). The trichocyst bodies were square in cross section and about 1.5–2 μm wide (Figs 32–34).

TEMs through cysts at the latest stages in development demonstrated an accumulation of fully differentiated zoospores, each delimited by an independent plasma membrane that was subtended by small alveoli (Figs 35, 42, and 43). Each zoospore contained dinoflagellate-like trichocysts (square in transverse section) and five major components: (1) a posterior

Figs 4–14. Differential interference light micrographs (DIC) showing a series of developmental stages associated with the intracellular infection and proliferation of *Parvilucifera prorocentri* within its host, *Prorocentrum fukuyoi*. **4**. The earliest stages of infection. Four or five parasitic cells (arrowheads) appear to be dividing within a sporangium (arrow). **5**. The proliferation of parasites within a sporangium (arrow). **6**. The growth of the parasitic sporangium (arrow), consisting of spherical bodies (arrowhead) and amorphous spaces (asterisk). **7**. Amorphous spaces (asterisk) within a growing undifferentiated sporangium and the formation of a multilayered cyst wall (arrow). **8**. The formation of a germ tube (arrow) derived from the cyst wall. **9**. A sporangium undergoing early stages of differentiation within the cyst wall (arrows). At this stage, the sporangium consists of an undifferentiated central mass (c) that is surrounded by a more granulated cytoplasm. **10**. The sporangium has differentiated into zoospores (arrowheads) and an open germ tube (arrow). Figs 4–10 are at the same scale (Scale bar = 10 μm). Inset: A high magnification DIC micrograph showing a free-swimming zoospore consisting of a posterior refractile body (arrowhead) and a transverse flagellum (arrow) (Inset Scale bar = 2 μm). **11**. A nearly empty cyst of *Parv. prorocentri* containing two motile zoospores (arrowheads). **12**. An empty cyst of *Parv. prorocentri*. Figs 11–12 are at the same scale (Scale bar = 10 μm). **13**. A double parasitic infection (arrows) within the cytoplasm of *P. fukuyoi*. **14**. The growth and proliferation of two parasitic sporangia (arrows) within the cytoplasm of *P. fukuyoi*. Figs 13 and 14 are at the same scale (Scale bar = 10 μm).

refractile body, (2) a central mitochondrion with tubular cristae, (3) lipid droplets, (4) a Golgi body consisting of six cisternae and (5) a relatively large nucleus (diam about 1.5 μm) with condensed chromatin localized beneath the nuclear envelope (Figs 35–38, 42, and 44). Each zoospore also possessed two flagella, one of which was a longer transverse (anterior) flagellum that wrapped around the cell body; the posterior flagellum was shorter and was not visible using light microscopy (Figs 10 inset, 42–44). The basal bodies of both flagella consisted of nine triplets and were oriented orthogonally to one another (Figs 47 and 48). A transverse septum was present in the transition zone between the basal body and the axoneme (Fig. 48). The axoneme of the anterior flagellum contained two central microtubules that were different in morphology; one was consistently

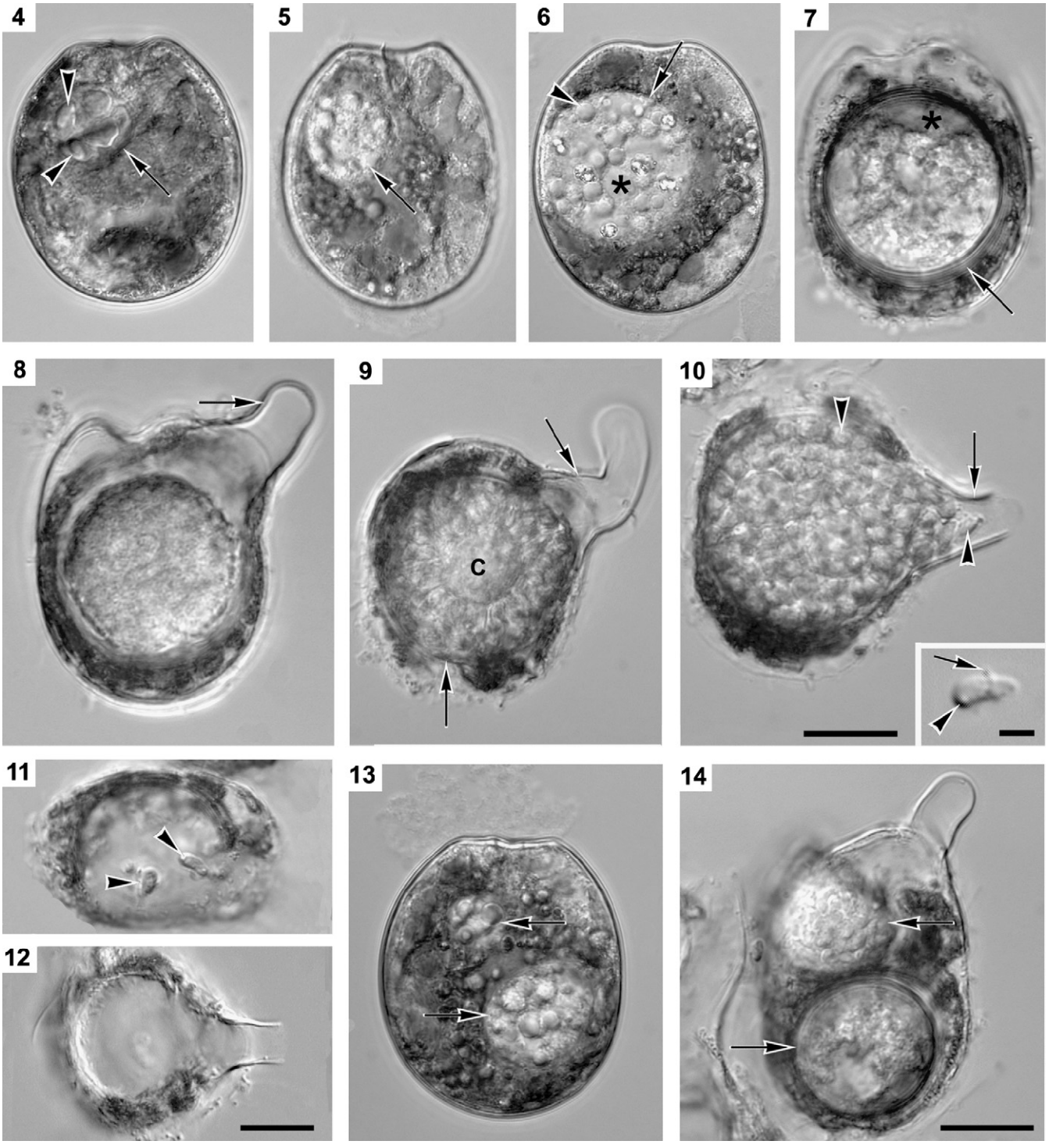

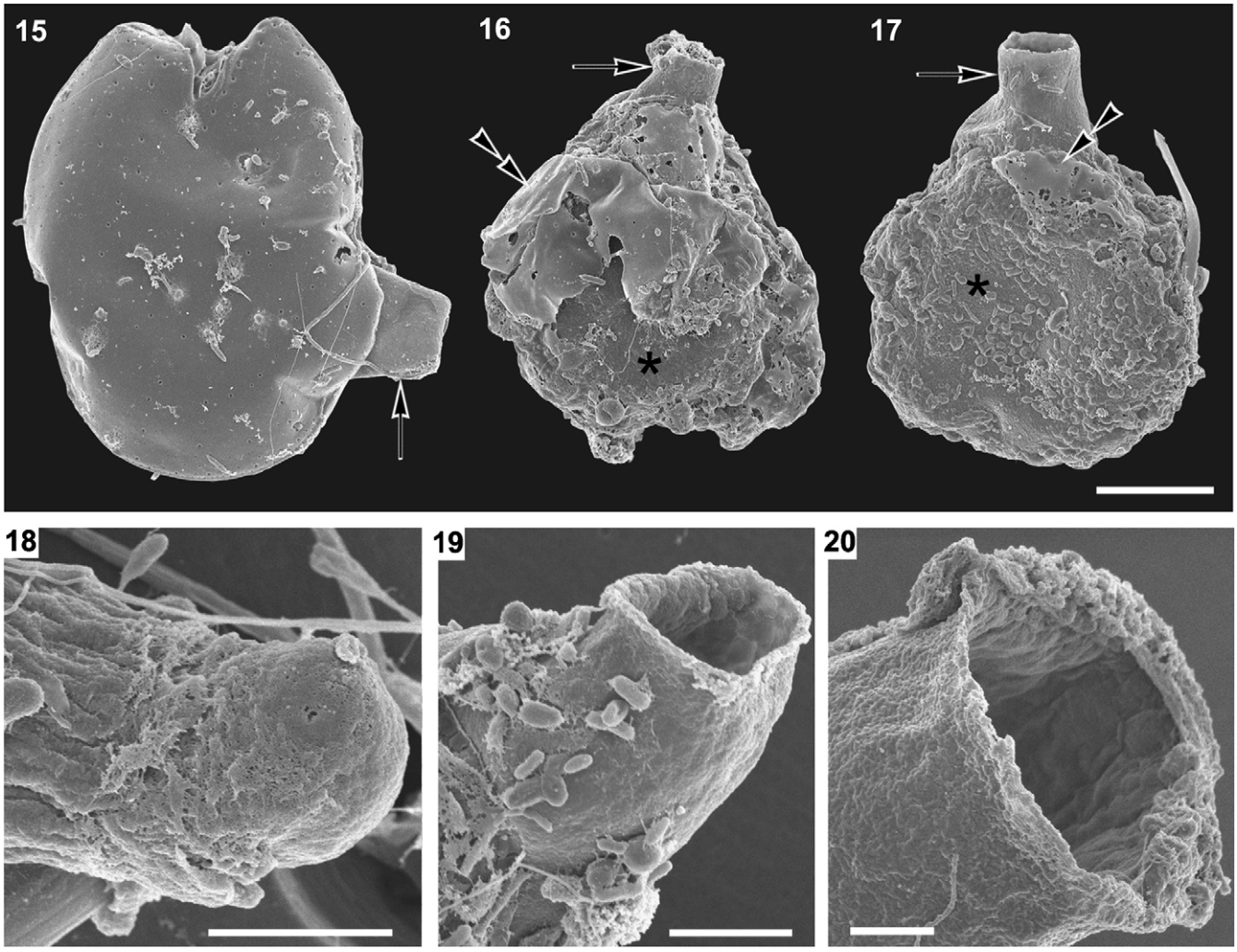

Fig. 15–20. Scanning electron micrographs (SEM) showing surface features of the cyst of *Parvilucifera prorocentri* within its host, *Prorocentrum fukuyoi*. **15**. The germ tube (arrow) of *Parv. prorocentri* emerges from the sagittal suture between the right (visible) and left thecal plates of the host. **16**. A late stage of cyst development showing the germ tube (arrow), the cyst wall (asterisk) and remnants of the host theca (double arrowheads). **17**. An empty cyst showing the germ tube (arrow), the cyst wall (asterisk) and remnants of the host theca (double arrowheads). Figs 15–17 are at the same scale (Scale bar = 10 μm). **18**. The tip of an unopened germ tube (Scale bar = 2.5 μm). **19**. The opening of a curved germ tube (Scale bar = 2.5 μm). **20**. The internal surface of a germ tube (Scale bar = 1 μm).

Figs 21–27. Transmission electron micrographs (TEM) of *Parvilucifera prorocentri* during the early to middle stages of development within its host, *Prorocentrum fukuyoi*. **21**. Tangential section through the sporangial envelope in an early stage of development showing its convoluted texture (Scale bar = 1 μm). **22–24**. Sections through an early sporangium showing a relatively undifferentiated cytoplasm containing lipid droplets (L) and surrounded by an envelope consisting of three layers: a thin outer layer (arrowhead), a convoluted middle layer (arrow) and a thick inner layer (double arrowheads) (H, host; P, parasite; Fig. 22, Scale bar = 2 μm; Fig. 23, Scale bar = 3 μm; Fig. 24, Scale bar = 0.5 μm). **25**. Section through a deteriorating host cell containing two sporangia. Remnants of the host are indicated by the presence of the thecal plates (double arroweads) and plastids (arrowheads). The two sporangia are in a mid-stage of development and consist of an indented wall (arrows), lipid droplets (L), nuclei (N) and amorphous spaces (asterisks) within a relatively undifferentiated cytoplasm (Scale bar = 3 μm). **26**. Section showing the cytoplasm of a sporangium in a mid-stage of development showing a nucleus (N), rough endoplasmic reticulum (arrows), a Golgi body (G) and mitochondria with tubular cristae (arrowheads) (Scale bar = 0.5 μm). **27**. Section showing the cytoplasm of a sporangium in a mid-stage of development showing lipid droplets (L) and trichocysts (double arrowheads) (arrow, anterior 'head' of trichocyst) (Scale bar = 0.5 μm).

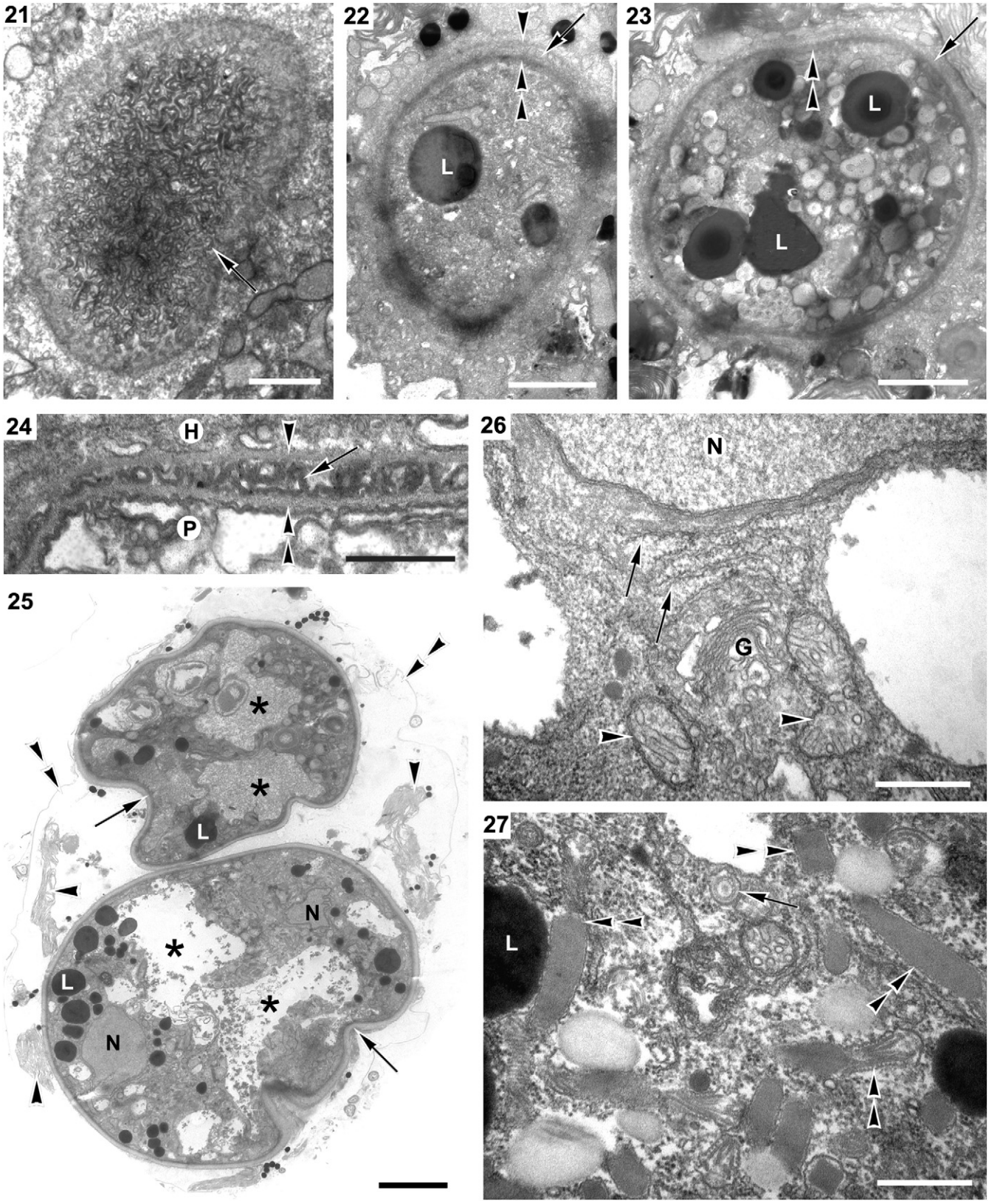

smaller than the other (Fig. 40). An inconspicuous pseudoconoid-like scaffold consisting of 4–5 microtubules was present near the apex of the zoospores (Figs 38–39, 41, 48). Each zoospore contained a cluster of pseudoconoid-associated micronemes and several linear trichocysts that were oriented toward the apex

of the cell (Figs 37, 41, 43, 46). A cluster of oblong microbodies, each enveloped by a membrane, was also observed near the cell apex of zoospores (Figs 44 and 45). An unambiguous apicoplast homologue was not observed.

Species description

Alveolata Cavalier-Smith, 1991
Myzozoa Cavalier-Smith et Chao, 2004
***Parvilucifera prorocentri* Leander and Hoppenrath sp. nov.**

Description

Biflagellate zoospores reniform, about 4 μm long and with transverse flagellum, small alveoli, refractile body, a central mitochondrion, one nucleus with condensed chromatin directly beneath the nuclear envelope, large lipid droplet(s), micronemes, bipartite trichocysts with bodies square in cross section that are oriented toward the cell apex and a cluster of oblong microbodies. A reduced, sheet-like pseudoconoid consisting of 4–5 microtubules positioned above an orthogonal pair of basal bodies. Early developmental stage of intracellular sporangium about 5–15 μm in diam that formed a complex three-layered envelope with a convoluted mid-layer surrounding spherical bodies and amorphous spaces; middle stages about 20–25 μm in diam and consisting of a robust cyst wall containing an undifferentiated mass; late stages consisting of a mass of differentiated zoospores. Pronounced germ tube about 4–5 μm in diam and 10–15 μm long. Prior to spore differentiation, the sporangia contain nuclei without condensed chromatin, mitochondria, lipid droplets, trichocysts and basal bodies.

Hapantotype

Both resin-embedded parasites used for TEM and parasites on gold sputter-coated SEM stubs have been deposited in the Beaty Biodiversity Research Centre (Marine Invertebrate Collection) at the University of British Columbia, Vancouver, Canada. The embedded parasites were fixed in situ within the host cells.

Type locality

Boundary Bay, British Columbia, Canada (49°0′N, 123°8′W).

Habitat

Marine.

Etymology for the specific epithet

Refers to the genus of the type dinoflagellate host, *Prorocentrum*.

Type host

Prorocentrum fukuyoi Murray et Nagahama (Alveolata, Myzozoa, Dinoflagellata, Prorocentrales).
Location in host. Within the cytoplasm.

Discussion

Intracellular development

The intracellular development of *Parv. prorocentri* is similar to that described for *Parv. infectans*, *Perkinsus* and syndineans, such as *Syndinium*, *Coccidinium* and *Amoebophrya* (Azevedo 1989; Azevedo et al. 1990; Chatton and Biecheler 1934, 1936; Fritz and Nass 1992; Manier et al. 1971; Maranda 2001; Norén et al. 1999). An infective zoospore enters a host cell (or host tissue in the case of *Perkinsus* and many syndineans) and develops into a vacuolated, undifferentiated sporangium that increases in size to about 20–25 μm before forming an enveloping cyst wall. The sporangial cytoplasm ultimately differentiates into many minute zoospores

Figs 28–34. Transmission electron micrographs (TEM) of *Parvilucifera prorocentri* during the middle to late stages of development within its host, *Prorocentrum fukuyoi*. **28**. Section through an almost fully developed cyst; note that the host cell has disintegrated leaving only remnants attached to the outside of the cyst wall (arrow). The contents within the cyst have become differentiated into nuclei (arrowheads), trichocysts (double arrowheads), amorphous spaces (asterisks) and several other structures that are more conspicuous at higher magnification. Elongated nuclei, possibly undergoing division, are apparent at this stage (triple arrowheads) (Scale bar = 3 μm). **29**. Section showing the cyst wall (W) and the cytoplasm containing flagellar axonemes (arrows), mitochondria with tubular cristae (M) and trichocysts (double arrowheads) (Scale bar = 0.5 μm). **30**. Section showing the cyst wall (W), subtending alveolar vesicles (arrowheads), mitochondria with tubular cristae (M) and a nucleus with minimal condensed chromatin (N) (Scale bar = 0.5 μm). **31**. Section showing two nuclei at a later stage in development and having a reticulated pattern of condensed chromatin (N) (Scale bar = 0.5 μm). **32**. Section showing two nuclei at the most mature stage in development and having a peripheral distribution of condensed chromatin and a central nucleolus (arrowheads) (Scale bar = 0.5 μm). **33–34**. Sections showing the general ultrastructure of the trichocysts (double arrowheads). Each trichocyst is surrounded by a membrane and consists of a main body (B) that is square in transverse section and a head region (H) (Scale bars = 0.2 μm).

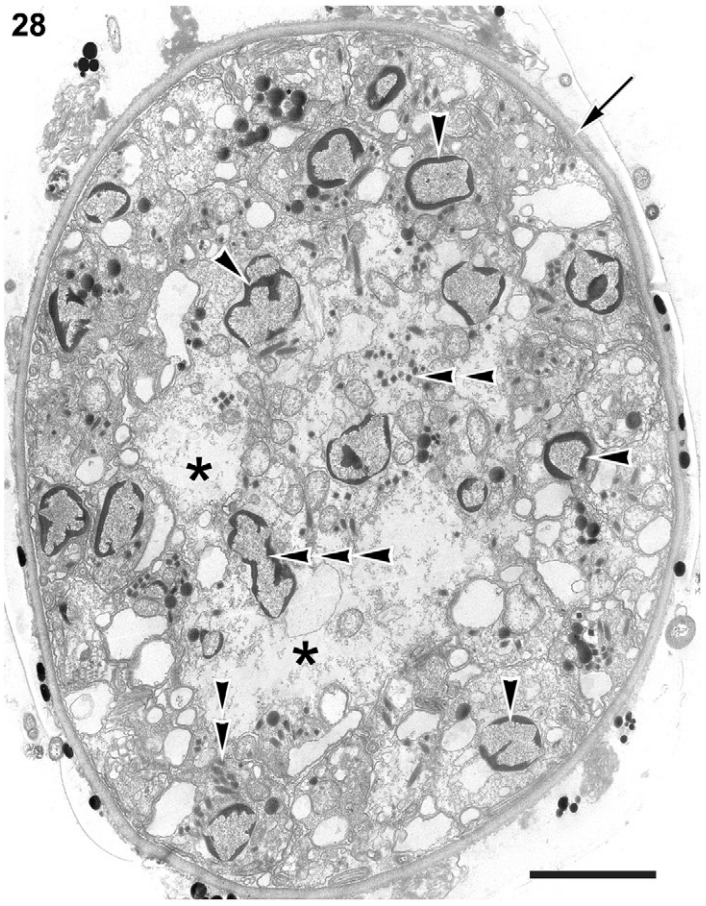
28

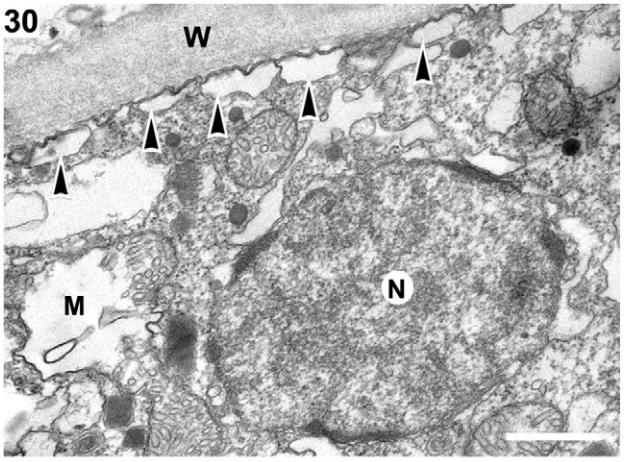
30
W
M
N

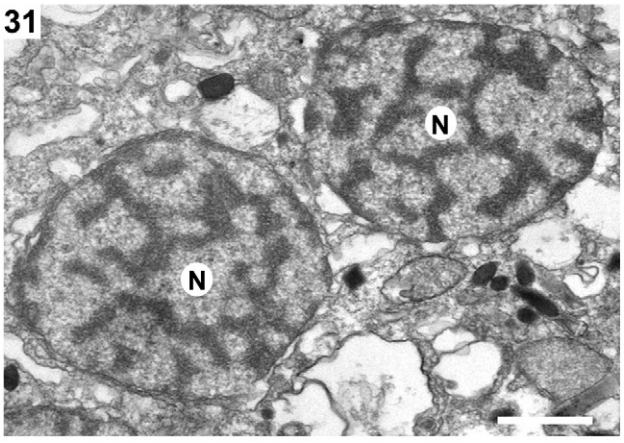
31
N
N

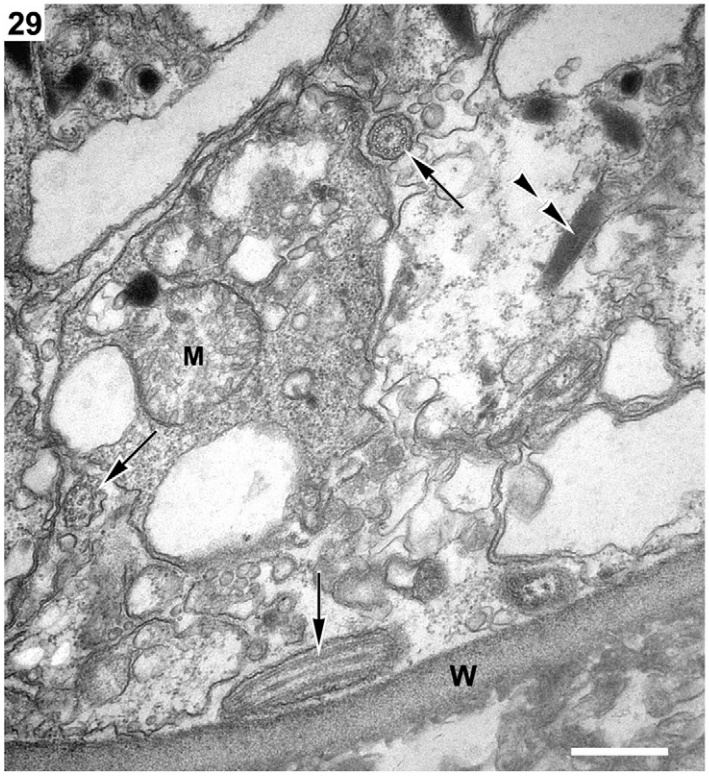
29
M
W

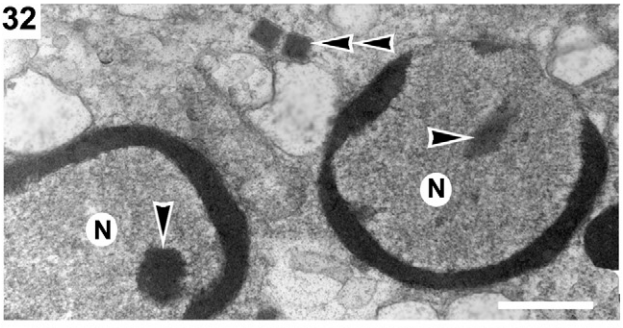
32
N
N

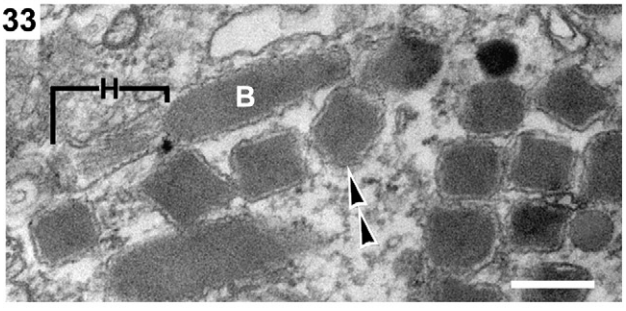
33
H
B

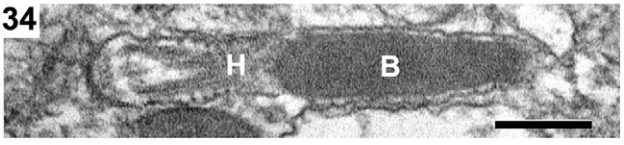
34
H
B

(3–20 μm) that escape one host in order to infect another one. Differences in the spatial organization of the developing zoospores, the ways in which the zoospores escape from the host, zoospore ultrastructure and features of the cyst wall are diagnostic for each of the genera and species listed above.

For instance, the structure of the sporangial envelope in *Parv. prorocentri* is different from that in *Parv. infectans*. In *Parv. infectans*, the cyst wall surface is ornamented with regularly arranged papillae (or warts) and incorporates several simple apertures through which the zoospores escape (Norén et al. 1999). By contrast, the sporangial envelope of *Parv. prorocentri* is relatively smooth, with an underlying convoluted layer during early developmental stages, and forms a robust germ tube, through which the zoospores escape. The pronounced germ tube of *Parv. prorocentri* is reminiscent of the weakly developed germ tube (syn. discharge tube) described in cultured *Perkinsus* (Azevedo 1989; Azevedo et al. 1990; Dungan and Reece 2006; Lester and Davis 1981; Perkins 1996; Perkins and Menzel 1967). As far as we know, germ tubes have not been described for syndineans, and different genera in this group use diverse strategies for releasing zoospores. The zoospores of *Amoebophrya*, for example, emerge and escape from a host during the dynamic expansion of a vermiform stage (Coats 1999; Fritz and Nass 1992; Gunderson et al. 2002). Moreover, differentiation of the zoospores in syndineans, like *Amoebophrya* and *Coccidinium*, takes place in highly organized arrays (e.g. beehive-like structures) that radiate from a central mass and subtend the cyst wall (Chatton and Biecheler 1934, 1936; Fritz and Nass 1992; Maranda 2001). This stands in contrast to *Parvilucifera* and *Perkinsus*, where the zoospores differentiate into a relatively unordered mass within the cyst. In *Parvilucifera infectans*, the cyst often disassociates from the decaying host before several hundred zoospores are released.

Zoospore morphology

The gross morphology of *Parv. prorocentri* zoospores is very similar to the zoospores described for *Parv. infectans*, *Perkinsus*, *Duboscquella*, syndineans and *Oxyrrhis*. The zoospores in all of these lineages are reniform with a rounded posterior end, possess a conspicuous refractile body (putative carbohydrate grain – absent in *Oxyrrhis*) and possess a transverse flagellum within a cingulum-like depression (the "dinokont" condition) (Appleton and Vickerman 1998; Azevedo 1989; Blackbourn et al. 1998; Brugerolle and Mignot 1979; Dodge and Crawford 1971a, b; Norén et al. 1999; Skovgaard et al. 2005). Like *Parv. infectans*, the zoospores of *Parv. prorocentri* possess a Golgi body with six cisternae and a short posterior flagellum that is essentially invisible under the light microscope (Norén et al. 1999). Moreover, the axoneme within the transverse (anterior) flagellum in both *Parv. prorocentri* and *Parv. infectans* has two central microtubules that differ in size: one singlet microtubule is reduced relative to the other (Norén et al. 1999). The two basal bodies in *Parv. prorocentri* are orthogonally arranged, composed of triplets and contain a transverse septum (syn. plate) at the transition zone. These features have also been described in *Parv. infectans*, *Perkinsus*, *Rastrimonas* (formerly *Cryptophagus*), *Voromonas* (formerly *Colpodella*), *Chilovora* (formerly *Colpodella* and *Spiromonas*), *Colponema* and *Oxyrrhis* (Brugerolle 2002, 2003; Brugerolle and Mignot 1979; Cavalier-Smith and Chao 2004; Dodge and Crawford 1971b; Mignot and Brugerolle 1975; Mylnikov 1991, 2000; Norén et al. 1999). However, unlike *Parv. infectans* and *Perkinsus*, a densely stained globule positioned proximal to the transverse septum is not observed in the basal bodies of *Parv. prorocentri*.

Demonstrating the presence of a pseudoconoid (syn. "open" conoid) in *Parv. prorocentri* was of paramount

Figs 35–41. Transmission electron micrographs (TEM) of *Parvilucifera prorocentri* during the latest stages of development within its host, *Prorocentrum fukuyoi*. **35**. Section through a fully developed cyst showing the cyst wall (arrow), the germ tube, and fully differentiated, mature zoospores containing a nucleus (arrowhead), a refractile body (R) and other structures that are best viewed at higher magnification (Scale bar = 4 μm). **36**. Section of an individual zoospore showing the enveloping plasma membrane (triple arrowhead), subtending alveolar vesicles (A), a posterior refractile body (R), a central mitochondrion with tubular cristae (M), two flagellar axonemes (arrows) and a nucleus with a peripheral pattern of condensed chromatin (N) (Scale bar = 1 μm). **37**. Section of an individual zoospore showing the enveloping plasma membrane (triple arrowhead), trichocyst-like extrusomes in longitudinal view (double arrowheads) and oriented toward the cell apex, a flagellar axoneme (arrow), a posterior refractile body (R) and a central mitochondrion with tubular cristae (M) (Scale bar = 1 μm). **38**. Section of an individual zoospore showing a posterior refractile body (R), a mitochondrion with tubular cristae (M), a nucleus with a peripheral pattern of condensed chromatin (N), square trichocysts in transverse section (double arrowheads), a Golgi body consisting of six cisternae (G) and an unidentified organelle (asterisk) positioned near a curved row of microtubules (arrowhead; possibly a reduced pseudoconoid) (Scale bar = 0.5 μm). **39**. Higher magnification TEM of the curved row of five microtubules (arrowheads) shown in Fig. 38 (Scale bar = 0.1 μm). **40**. Cross-section of the anterior (flagellar) axoneme showing two central microtubules with different morphology; one is smaller (arrowhead) than the other (Scale bar = 0.1 μm). **41**. Section showing a curved sheet of 4–5 microtubules (arrowhead, putative conoid), a cluster of micronemes in transverse section (arrow) and several trichocysts in transverse section (double arrowheads, square profiles of the trichocyst bodies; triple arrowheads, circular profiles of the trichocyst heads) (Scale bar = 0.2 μm).

interest and it was extensively searched for under the TEM. Our observations suggest that the pseudoconoid in *Parv. prorocentri* is inconspicuous, consists of only 4–5 microtubules with an associated cluster of micronemes and is positioned directly above the orthogonal basal bodies. This configuration is most similar to that described in *Parv. infectans* and *Rastrimonas* (Brugerolle 2002, 2003; Norén et al. 1999). The simplest pseudoconoid described so far is found in *Parv. infectans,* which like *Parv. prorocentri*, also consists of 4–5 microtubules arranged in a "C-shaped" configuration (Norén et al. 1999). Interestingly, an enigmatic lineage of parasitic

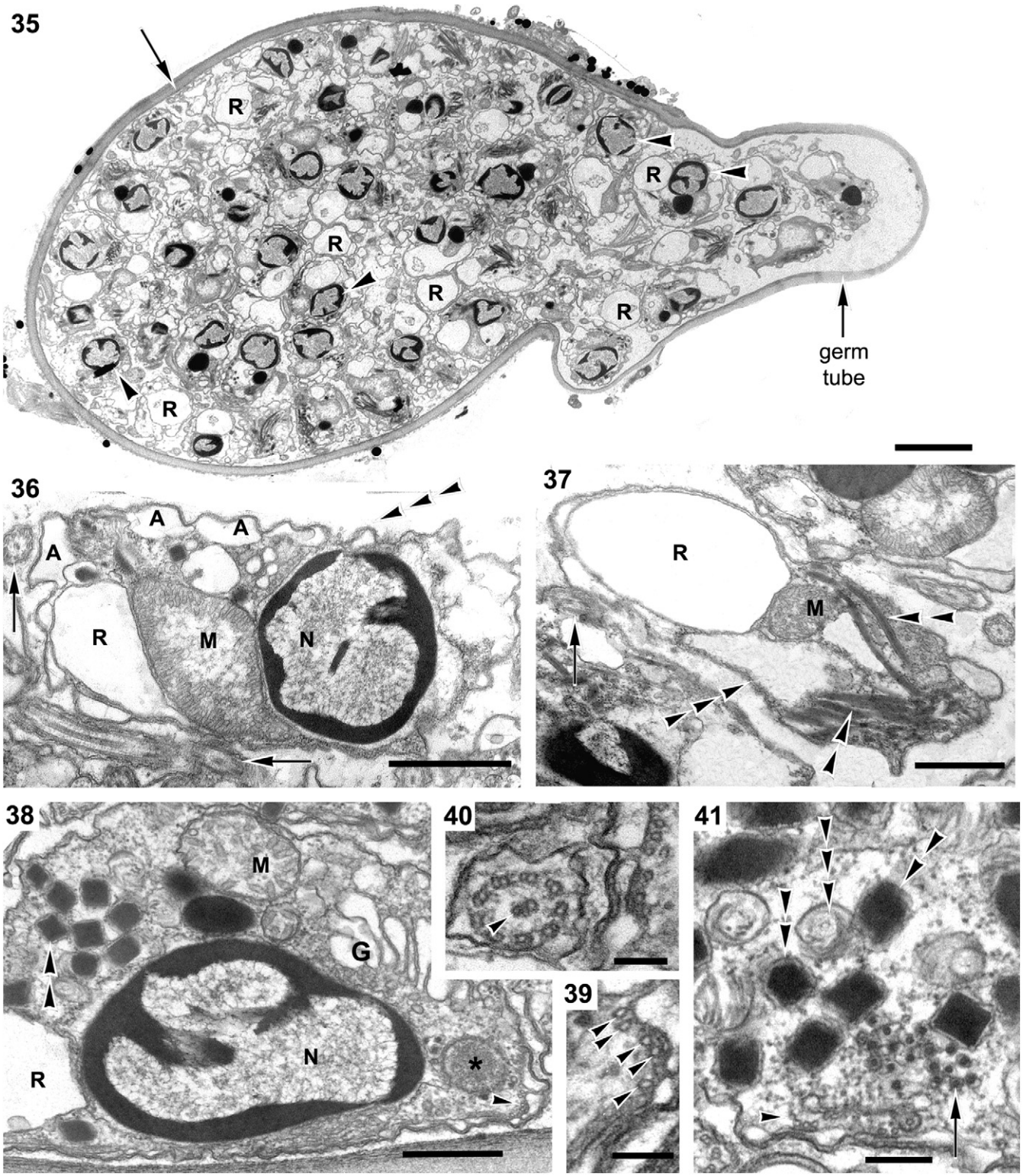

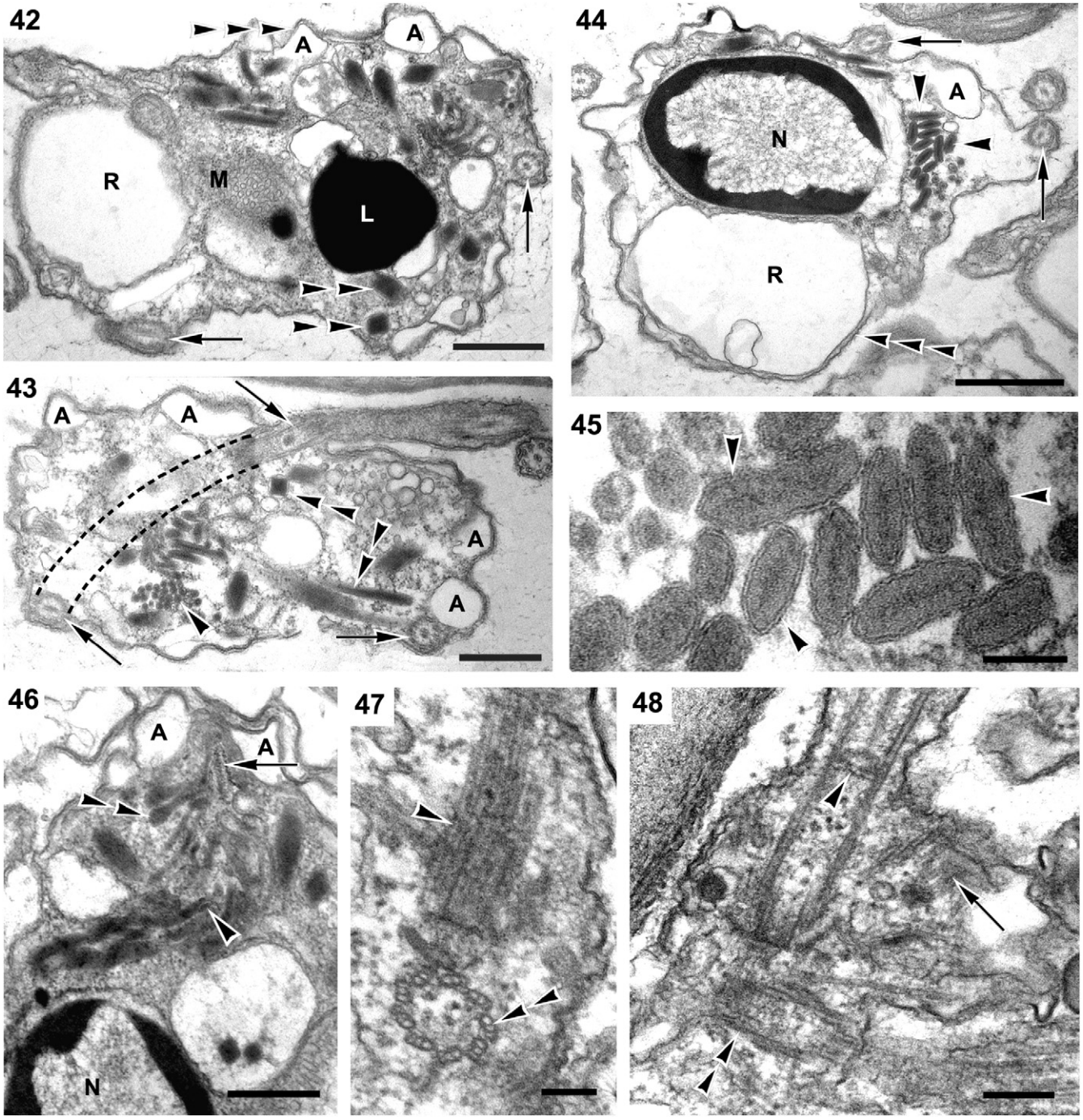

Figs 42–48. High magnification transmission electron micrographs of the zoospores of *Parvilucifera prorocentri*. **42**. Section of an individual zoospore showing the enveloping plasma membrane (triple arrowhead), subtending alveolar vesicles (A), a posterior refractile body (R), a central mitochondrion with tubular cristae (M), a relatively large lipid droplet (L), two flagellar axonemes (arrows) and trichocysts (double arrowheads) (Scale bar = 0.5 μm). **43**. Section of an individual zoospore showing alveolar vesicles (A), trichocysts (double arrowheads), flagella (arrows) and the profiles of a cluster of pseudoconoid-associated micronemes (arrowhead). Dashed lines indicate the course of the transverse, anterior flagellum (Scale bar = 0.5 μm). **44**. Section of an individual zoospore showing the enveloping plasma membrane (triple arrowhead), a subtending alveolar vesicle (A), a refractile body (R), two flagellar axonemes (arrows), a nucleus with a peripheral pattern of condensed chromatin (N) and oblong microbodies (arrowheads) (Scale bar = 1 μm). **45**. Section showing the oblong microbodies, each of which is surrounded by a membrane (arrowheads) (Scale bar = 0.1 μm). **46**. Section of the anterior end of an individual zoospore showing alveolar vesicles (A), a nucleus (N), an inconspicuous profile of the pseudoconoid (arrow), trichocysts (arrowhead) and micronemes with bulbous posterior ends (double arrowheads) oriented toward the apex of the cell (Scale bar = 0.5 μm). **47**. Section of the flagellar insertions showing a basal body in transverse section with nine triplets (double arrowheads) that is oriented orthogonally to the second basal body (arrowhead) (Scale bar = 0.1 μm). **48**. Section of the flagellar insertions showing a basal body in oblique longitudinal section (double arrowheads) and a basal body in longitudinal section containing a transverse septum in the transition zone (arrowhead). A section through the 4–5 microtubules of the pseudoconoid (arrow) is also shown (Scale bar = 0.1 μm).

flagellates of hemichordates, namely *Acrocoelus*, appears to lack a pseudoconoid altogether while still maintaining other components of the apical complex, such as rhoptries, micronemes and other secretory organelles (Fernández et al. 1999a, b). More robust pseudoconoids are present in *Perkinsus* and several "free-living" predatory flagellates, such as *Colpodella*, *Voromonas* and *Chilovora* (Brugerolle and Mignot 1979; Leander et al. 2003; Mylnikov 1991, 2000; Mylnikov et al. 1998; Perkins 1976, 1996; Simpson and Patterson 1996). The relatively robust pseudoconoids in these taxa function in cell penetration during parasitic invasions and myzocytosis-based modes of feeding. The reduced pseudoconoids in *Parv. infectans* and *Parv. prorocentri* might reflect a different mechanism of intracellular invasion. For instance, our observations indicate that *Parv. prorocentri* enters its dinoflagellate host through the relatively large flagellar pore, or the accessory pore, found in the periflagellar area of the Prorocentrales. Exploitation of this weak point in the host's armor is a mechanism of invasion that is significantly different from a mechanism that requires direct penetration through the host's cell surface.

Extrusomes

Different types of apical complex-associated extrusomes, in addition to rhoptries and micronemes, have been described in several myzozoans. For example, *Acrocoelus* possesses tri-layered spherical organelles that are considerably more complex than rhoptries and micronemes (Fernández et al. 1999a). Although homologues for these organelles are not known, the suggestion has been made that they might be related to the so-called "toxicysts" of *Colponema* (Fernández et al. 1999a; Mignot and Brugerolle 1975). Similarly, the zoospores of *Parv. prorocentri* possess a cluster of ovoid, membrane-bound "microbodies" that appear to be novel and without an obvious function. The zoospores of *Parv. prorocentri* also possess several bipartite, square-bodied trichocysts that are frequently oriented toward the cell apex. Nearly identical trichocysts have been described in *Oxyrrhis*, "core" dinoflagellates and in the zoospores of syndineans, *Duboscquella, Voromonas*, *Chilovora* and *Alphamonas* (Brugerolle and Mignot 1979; Cavalier-Smith and Chao 2004; Dodge and Crawford 1971a; Fritz and Nass 1992; Harada et al. 2007; Leander et al. 2003; Manier et al. 1971; Mylnikov 1991, 2000; Mylnikov et al. 1998; Skovgaard et al. 2005). Interestingly, bipartite trichocysts are absent in *Perkinsus*, *Parv. infectans* and colpodellids *sensu stricto* (Azevedo 1989; Blackbourn et al. 1998; Cavalier-Smith and Chao 2004; Norén et al. 1999). The "toxicysts" in *Colponema* are similar in gross morphology to the bipartite trichocysts and are probably homologous (Mignot and Brugerolle 1975). Nonetheless, once the backbone of the myzozoan radiation has been satisfactorily resolved, it should be possible to address (1) whether bipartite trichocysts are synapomorphic for a large myzozoan or more inclusive alveolate clade (e.g. the "Dinozoa" Cavalier-Smith 1981, emend Cavalier-Smith and Chao 2004) and (2) the hypothesis that the bipartite dinoflagellate-like trichocysts are derived from rhoptry-like precursors.

Group I alveolates?

As described above, *Parv. prorocentri* possesses a combination of features found in *Parv. infectans* (e.g. dinoflagellate hosts and ultrastructural similarities in the sporangia, Golgi, flagellar apparatus and apical complex), *Perkinsus* (e.g. germ tubes) and syndineans (e.g. bipartite trichocysts and nuclear ultrastructure). The nuclei in the mature zoospores of *Parv. prorocentri* and syndineans (e.g. *Amoebophrya* and *Syndinium*) are essentially identical in possessing a conspicuous nucleolus and condensed chromatin positioned peripherally beneath the nuclear envelope (Fritz and Nass 1992; Manier et al. 1971). The condensed chromatin within these nuclei does not correspond to chromosomes as seen in *Oxyrrhis* and the "core" dinoflagellates (Dodge and Crawford 1971a; Holland 1974; Ris and Kubai 1974; Soyer 1974). This nuclear ultrastructure is also somewhat similar to that described for *Perkinsus* (Azevedo 1989; Blackbourn et al. 1998), but significantly different from the nuclei of *Parv. infectans*, which lack condensed chromatin and consist of circumferential layers of thin fibers (Norén et al. 1999).

The zoospores of syndineans and perkinsids are of the order of 3–20 μm long, and they appear to be widely distributed throughout the oceans. Therefore, it is not surprising that environmental sequencing surveys of nanoeukaryotes (2–20 μm) have generated sequences from a diverse assemblage of parasitic alveolates, especially syndineans (Group II alveolates) and the so-called "Group I" alveolates, which have yet to be fully characterized at the cellular level. Molecular phylogenies have shown that both Group I alveolates and syndineans tend to branch as sister groups to the clade consisting of *Oxyrrhis* and the "core" dinoflagellates; moreover, perkinsids tend to branch as the nearest sister group to the clade consisting of Group I alveolates, syndineans and "core" dinoflagellates (Diez et al. 2001; Dolven et al. 2007; Groisillier et al. 2006; Harada et al. 2007; López-García et al. 2001; Moon-van der Staay et al. 2001; Moreira and López-García 2002; Takishita et al. 2007; Worden 2006). Because *Parv. prorocentri* possesses a combination of ultrastructural characters found in perkinsids and syndineans, these parasites constitute an intriguing candidate for discovering the

cellular identity of a major subclade of Group I alveolates. Needless to say, molecular phylogenetic data from *Parv. prorocentri* will enable us to evaluate this hypothesis more rigorously. However, the eventual acquisition of these molecular data is unpredictable.

Host specificity and the life cycle stages that might exist between host infections are not well understood in syndineans, perkinsids and *Parv. prorocentri*. It is possible that host specificity is a species-specific characteristic that will be reflected in tree topologies derived from molecular phylogenetic analyses. However, like *Parv. prorocentri*, some syndineans such as *Amoebophrya* also infect *Prorocentrum* species (Maranda 2001), and *Parv. infectans* was shown to be capable of infecting several different phototrophic dinoflagellates (Norén et al. 1999). Overall, the known host specificity and the combination of ultrastructural characteristics in *Parv. prorocentri* (described above) indicate that these parasites are most similar to *Parv. infectans* and are more distantly related to colpodellids *sensu stricto* and apicomplexan parasites (syn. "Sporozoa" *sensu* Cavalier-Smith 1999). Although *Parv. prorocentri* differs from *Parv. infectans* in having bipartite trichocysts, *Perkinsus*-like germ tubes and syndinean-like nuclei, we have decided not to erect a new genus name at this stage. Presumably, molecular phylogenetic data from this species will provide additional insights into early myzozoan relationships and systematics. Nonetheless, the emerging fact that molecular sequences from syndineans, perkinsids and Group I alveolates are frequently generated in marine environmental sequencing surveys, indicates that these parasites are abundant in marine ecosystems and that the overall diversity of myzozoan parasites is still just beginning to be explored and appreciated.

Acknowledgments

This work was supported by a scholarship to M. H. from the Deutsche Forschungsgemeinschaft (Grant Ho3267/1-1) and funds from the National Science Foundation – Assembling the Tree of Life (NSF #EF-0629624), the National Science and Engineering Research Council of Canada (NSERC 283091-04) and the Canadian Institute for Advanced Research, Programs in Evolutionary Biology and Integrated Microbial Biodiversity.

References

Appleton, P.L., Vickerman, K., 1998. *In vitro* cultivation and developmental cycle in culture of a parasitic dinoflagellate (*Hematodinum* sp.) associated with mortality of the Norway lobster (*Nephrops norvegicus*) in British waters. Parasitology 116, 115–130.

Azevedo, C., 1989. Fine structure of *Perkinsus atlanticus* n. sp. (Apicomplexa, Perkinsea) parasite of the clam *Ruditapes decussatus* from Portugal. J. Parasitol. 75, 627–635.

Azevedo, C., Corral, L., Cachola, R., 1990. Fine structure of zoosporulation in *Perkinsus atlanticus* (Apicomplexa: Perkinsea). Parasitology 100, 351–358.

Blackbourn, J., Bower, S.M., Meyer, G.R., 1998. *Perkinsus qugwadi* sp. nov. (incertae sedis), a pathogenic protozoan parasite of Japanese scallops, *Patinopecten yessoensis*, cultured in British Columbia, Canada. Can. J. Zool. 76, 942–953.

Brugerolle, G., 2002. *Cryptophagus subtilis*: a new parasite of cryptophytes affiliated with the Perkinsozoa lineage. Eur. J. Protistol. 37, 379–390.

Brugerolle, G., 2003. Apicomplexan parasite *Cryptophagus* renamed *Rastrimonas* gen. nov. Europ. J. Protistol. 39, 101.

Brugerolle, G., Mignot, J.P., 1979. Observations sur le cycle l'ultrastructure et la position systématique de Spiromonas perforans (*Bodo perforans* Hollande, 1938), flagellé parasite de *Chilomonas paramecium*: ses relations avec les dinoflagellés et sporozoaires. Protistologica 15, 183–196.

Cachon, J., Cachon, M., 1987. Parasitic dinoflagellates. In: Taylor, F.J.R. (Ed.), The Biology of Dinoflagellates. Blackwell Science Publishers, Oxford, pp. 571–610.

Cavalier-Smith, T., Chao, E.E., 2004. Protalveolate phylogeny and systematics and the origins of Sporozoa and dinoflagellates (phylum Myzozoa nom. nov.). Eur. J. Protistol. 40, 185–212.

Chatton, É., Biecheler, B., 1934. Les Coccidnidae, Dinoflagellés coccodiomorphes parasites de Dinoflagellés, et le phylum des Phytodinozoa. C. R. Acad. Sci., Paris. 199, 252–255.

Chatton, É., Biecheler, B., 1936. Documents nouveaux relatifs aux Coccidinides (Dinoflagellés parasites). La sexualité du *Coccidinium mesnili* n. sp. C. R. Acad. Sci., Paris. 203, 573–576.

Coats, D.W., 1999. Parasitic life styles of marine dinoflagellates. J. Eukaryot. Microbiol. 46, 402–409.

Diez, B., Pedros-Alio, C., Massana, R., 2001. Study of genetic diversity of eukaryotic picoplankton in different oceanic regions by small-subunit rRNA gene cloning and sequencing. Appl. Environ. Microbiol. 67, 2932–2941.

Dodge, J.D., Crawford, R.M., 1971a. Fine structure of the dinoflagellate *Oxyrrhis marina*: I. The general structure of the cell. Protistologica 7, 295–304.

Dodge, J.D., Crawford, R.M., 1971b. Fine structure of the dinoflagellate *Oxyrrhis marina*: II. The flagellar system. Protistologica 7, 399–409.

Dolven, J.K., Lindqvist, C., Albert, V.A., Bjørklund, K.R., Yuasa, T., Takahashi, O., Mayama, S., 2007. Molecular diversity of alveolates associated with neritic north atlantic radiolarians. Protist 158, 65–76.

Dungan, C.F., Reece, K.S., 2006. In vitro propagation of two *Perkinsus* spp. parasites from Japanese manila clams *Venerupis philippinarum* and description of *Perkinsus honshuensis* n. sp. J. Eukaryot. Microbiol. 53, 316–326.

Fernández, I., Pardos, F., Benito, J., Arroyo, N.L., 1999a. *Acrocoelus glossobalani* gen. nov. et sp. nov., a protistan

flagellate from the gut of the enteropneust *Glossabalanus minutus*. Europ. J. Protistol. 35, 55–65.

Fernández, I., Arroyo, N.-L., Pardos, F., Benito, J., 1999b. Penetration into the gut cells of an enteropneust by the flagellate *Acrocoelus glossobalani* Fernandez et al., 1999. Eur. J. Protistol. 35, 255–263.

Fritz, L., Nass, M., 1992. Development of the endoparasitic dinoflagellate *Amoebophrya ceratii* within host dinoflagellate species. J. Phycol. 28, 312–320.

Groisillier, A., Massana, R., Valentin, K., Vaulot, D., Guilloul, L., 2006. Genetic diversity and habitats of two enigmatic marine alveolate lineages. Aqu. Micro. Ecol. 42, 277–291.

Gunderson, J.H., Shinu, J.A., Bowman II, W.C., Coats, D.W., 2002. Multiple strains of the parasitic dinoflagellate *Amoebophrya* exist in Chesapeake Bay. J. Eukaryot. Microbiol. 49, 469–474.

Harada, A., Ohtsuka, S., Horiguchi, T., 2007. Species of the parasitic genus *Duboscquella* are members of the enigmatic Marine Alveolate Group 1. Protist 158, 337–347.

Holland, A., 1974. Étude comparée de la mitose syndinienne, de celle des péridiens libres et des hypermastigines; infrastructure et cycle évolutif des syndinides parasites de radiolaires. Protistologica 10, 413–451.

Hoppenrath, M., Leander, B.S., 2006. Dinoflagellate, euglenoid, or cercomonad? The ultrastructure and molecular phylogenetic position of *Protaspis grandis* n. sp. J. Eukaryot. Microbiol. 53, 327–342.

Kuvardina, O.N., Leander, B.S., Aleshin, V.V., Mylnikov, A.P., Keeling, P.J., Simdyanov, T.G., 2002. The phylogeny of colpodellids (Eukaryota, Alveolata) using small subunit rRNA genes suggests they are the free-living ancestors of apicomplexans. J. Eukaryot. Microbiol. 49, 498–504.

Leander, B.S., Keeling, P.J., 2003. Morphostasis in alveolate evolution. Trends Ecol. Evol. 18, 395–402.

Leander, B.S., Keeling, P.J., 2004. Early evolutionary history of dinoflagellates and apicomplexans (Alveolata) as inferred from hsp90 and actin phylogenies. J. Phycol. 40, 341–350.

Leander, B.S., Kuvardina, O.N., Aleshin, V.V., Mylnikov, A.P., Keeling, P.J., 2003. Molecular phylogeny and surface morphology of *Colpodella edax* (Alveolata): insights into the phagotrophic ancestry of apicomplexans. J. Eukaryot. Microbiol. 50, 334–340.

Lester, R.J.G., Davis, G.H.G., 1981. A new *Perkinsus* species (Apicomplexa, Perknisidae) from the abalone *Haliotis ruber*. J. Invert. Path. 37, 181–187.

López-García, P., Rodriguez-Valera, F., Pedros-Alio, C., Moreira, D., 2001. Unexpected diversity of small eukaryotes in deep-sea antarctic plankton. Nature 409, 603–607.

Manier, J.-F., Fize, A., Grizel, H., 1971. *Syndinium gammari* n. sp. péridinien Duboscquodinida Syndinidae, parasite de *Gammarus locusta* (Lin.) Crustacé amphipode. Protistologica 7, 213–219.

Maranda, L., 2001. Infection of *Prorocentrum minimum* (Dinophyceae) by the parasite *Amoebophrya* sp. (Dinoflagellata). J. Phycol. 37, 245–248.

Mignot, J.P., Brugerolle, G., 1975. Étude ultrastructurale du flagellé phagotrophe *Colponema loxodes* Stein. Protistologica 11, 429–444.

Moon-van der Staay, S.Y., De Wachter, R., Vaulot, D., 2001. Oceanic 18S rDNA sequences from picoplankton reveal unsuspected eukaryotic diversity. Nature 409, 607–610.

Moreira, D., López-García, P., 2002. The molecular ecology of microbial eukaryotes unveils a hidden world. Trends Microbiol. 10, 31–38.

Murray, S., Nagahama, Y., Fukuyo, Y., 2007. A phylogenetic study of benthic, spine-bearing prorocentroids, including *Prorocentrum fukuyoi* sp. nov. Phycol. Res. 55, 91–102.

Mylnikov, A.P., 1991. The ultrastructure and biology of some representatives of order Spiromonadida (Protozoa). Zoologichesky Zhurnal 70, 5–15.

Mylnikov, A.P., 2000. The new marine carnivorous flagellate *Colpodella pontica* (Colpodellida, Protozoa). Zoologichesky Zhurnal 79, 261–266.

Mylnikov, A.P., Mylnikova, Z.M., Tsvetkov, A.I., 1998. The fine structure of carnivorous flagellate *Colpodella edax*. Biologiya Vnutrenich Vod. Sank-Ptersburg. 3, 55–62.

Norén, F., Moestrup, O., Rehnstam-Holm, A.-S., 1999. *Parvilucifera infectans* Norén et Moestrup sp. nov. (Perkinsozoa phylum nov.): a parasitic flagellate capable of killing toxic microalgae. Europ. J. Protistol. 35, 233–254.

Park, M.G., Yih, W., Coats, W., 2004. Parasites and phytoplankton, with special emphasis on dinoflagellate infections. J. Eukaryot. Microbiol. 51, 145–155.

Perkins, F.O., 1976. Zoospores of the oyster pathogen, *Dermocystidium marinum*. I. Fine structure of the conoid and other sporozoan-like organelles. J. Parasitol. 62, 959–974.

Perkins, F.O., 1996. The structure of *Perkinsus marinus* (Mackin, Owen and Collier, 1950) Levine, 1978 with comments on the taxonomy and phylogeny of *Perkinsus* spp. J. Shell. Res. 15, 67–87.

Perkins, F.O., Menzel, R.W., 1967. Ultrastructural sporulation in the oyster pathogen *Dermocystidium marinum*. J. Shell. Res. 15, 67–87.

Ris, H., Kubai, D.F., 1974. An unusual mitotic mechanism in the parasitic protozoan *Syndinium* sp. J. Cell Biol. 60, 702–720.

Saldarriaga, J.F., McEwan, M.L., Fast, N.M., Talyor, F.J.R., Keeling, P.J., 2003. Multiple protein phylogenies show that *Oxyrrhis marina* and *Perkinsus marinus* are early branches of the dinoflagellate lineage. Int. J. Syst. Evol. Microbiol. 53, 355–365.

Saldarriaga, J.F., Taylor, F.J.R., Cavalier-Smith, T., Menden-Deuer, S., Keeling, P.J., 2004. Molecular data and the evolutionary history of dinoflagellates. Eur. J. Protistol. 40, 85–111.

Siddall, M.E., Reece, K.S., Graves, J.E., Burreson, E.M., 1997. "Total evidence" refutes the inclusion of *Perkinsus* species in the phylum Apicomplexa. Parasitology 115, 165–176.

Siddall, M.E., Reece, K.S., Nerad, T.A., Burreson, E.M., 2001. Molecular determination of the phylogenetic position of a species in the genus *Colpodella*. Am. Mus. Nov. 3314, 1–10.

Simpson, A.G.B., Patterson, D.J., 1996. Ultrastructure and identification of the predatory flagellate *Colpodella pugnax* Cienkowski (Apicomplexa) with a description of *Colpodella turpis* n. sp. and a review of the genus. Syst. Parasitol. 33, 187–198.

Skovgaard, A., Massana, R., Balagué, V., Saiz, E., 2005. Phylogenetic position of the copepod-infesting parasite *Syndinium turbo* (Dinoflagellata, Syndinea). Protist 156, 413–423.

Soyer, M.-O., 1974. Étude ultrastructurale de *Syndinium* sp. Chatton, parasite coelomique de copépodes pélagiques. Vie Milieu 24, 191–212.

Takishita, K., Tsuchiya, M., Kawato, M., Oguri, K., Kitazato, H., Maruyama, T., 2007. Genetic diversity of microbial eukaryotes in anoxic sediment of the saline meromictic lake Namako-ike (Japan): on the detection of anaerobic or anoxic-tolerant lineages of eukaryotes. Protist 158, 51–64.

Uhlig, G., 1964. Eine einfache Methode zur Extraktion der vagilen, mesopsammalen Mikrofauna. Helgol. Wiss. Meeresunters. 11, 178–185.

Worden, A.Z., 2006. Picoeukaryote diversity in coastal waters of the Pacific Ocean. Aqu. Micro. Ecol. 43, 165–175.